

# Spatio-temporal analysis of sediment yield with a physically based model for a data-scarce headwater in Konya Closed Basin, Turkey

Cihangir Koycegiz, Meral Buyukyildiz and Serife Yurdagul Kumcu

## ABSTRACT

There are many empirical, semi-empirical and mathematical methods that have been developed to estimate sediment yield by researchers. In the last decades, the advancement in computer technologies has increased the use of mathematical models as they can solve the system more rapidly and accurately. The Soil and Water Assessment Tool (SWAT) is one of the physically based hydrological models that is preferred to compute sediment yield. In this study, spatial and temporal analysis of sediment yield in the Çarşamba Stream located at the Konya Closed Basin has been investigated using the SWAT model. Streamflow and sediment data collected during the 2003–2015 time period have been used in the analysis. Consequently, the SWAT presented satisfactory results compared with  $R^2 = 0.68$ , Nash–Sutcliffe Efficiency (NSE) = 0.68 in calibration and  $R^2 = 0.76$ , NSE = 0.66 in validation. According to the model results, spatial asymmetry in terms of sediment yield was determined in the sub-basins of the study area.

**Key words** | sediment, sediment rating curve, SUFI-2, SWAT

**Cihangir Koycegiz**  
**Meral Buyukyildiz** (corresponding author)  
Department of Civil Engineering,  
Konya Technical University,  
Konya,  
Turkey  
E-mail: [mbuyukyildiz@ktun.edu.tr](mailto:mbuyukyildiz@ktun.edu.tr)

**Serife Yurdagul Kumcu**  
Department of Civil Engineering,  
Necmettin Erbakan University,  
Konya,  
Turkey

## HIGHLIGHTS

- To establish, calibrate and validate a physically based model for the study area.
- To analyze sediment movement spatially and temporally.
- To suggest strategies for controlling sediment movement to authorities.

## INTRODUCTION

Only 3% of the water in the world can be used by humans. Water resources are rapidly decreasing due to industrialization, population growth, water pollution, unknown water consumption and climate change. This makes it important to plan, design and manage water structures correctly to use the available water resources most efficiently. Sediment transported in rivers and accumulated at the upstream of dam reservoirs reduces the economic life of the water structures and this accumulation is a serious problem and has

severe consequences for water management, flood control, producing energy, irrigation and drainage systems, domestic water supplies, river transportation systems and recreation works. Additionally, the morphology and ecology of the river are affected negatively by sediment. Due to the strong relationship between sustainability of water resources management and development of water resources, the estimation of sediment transport rate along the rivers and erosion control in the streams and tributaries is very important (Öztürk *et al.* 2001; Sivakumar 2006; Dogan 2009).

Sedimentation accumulation in dam reservoirs as a result of erosion from catchments during relatively short periods of flood discharges and also the gradual accumulation of the

This is an Open Access article distributed under the terms of the Creative Commons Attribution Licence (CC BY 4.0), which permits copying, adaptation and redistribution, provided the original work is properly cited (<http://creativecommons.org/licenses/by/4.0/>).

doi: 10.2166/ws.2021.016

incoming sediment load from a river basin emerge as an important problem as this decreases the economic life of dam reservoirs. The worldwide loss in reservoir storage capacity is reported to be approximately 1.0% per annum (Mahmood 1987). If the sediment transport rate is high, sediment will eventually fill a reservoir earlier than its economic life. It is estimated that on a worldwide basis the cost of the annual capacity loss because of the siltation is around US \$6 billion (Mahmood 1987). In Turkey, the lack of measurements taken for land use and erosion control results in the deposition of sediments and loss of capacity of dam reservoirs (Medik Dam, Akkaya Dam, Cubuk-I Dam, etc.).

It is very difficult to calculate the sediment yield analytically because of the complexity of phenomena affected by many parameters and resulting from geological, topographical and climatological factors. Although the measurements taken by sediment observation stations are the most reliable data, these may have disadvantages in cost and time. Generally, suspended sediment measurements are observed along the river on any day of each month, this causes a limited number of sediment data. In addition to direct measurement along the river, sediment load can also be estimated by rating curve method, regression analysis, artificial neural network (ANN) and empirical methods. The Soil and Water Assessment Tool (SWAT) is one of the physical-based tools used in estimating sediment transport rate. Although SWAT has been widely used for streamflow, there is a scarcity of literature applicable to the accuracy of sediment simulations (Borah & Bera 2003; Azzellino *et al.* 2015; Zeiger & Hubbard 2016; Ricci *et al.* 2018; Kesikoglu *et al.* 2019; Akar & Aksoy 2020; Yuan & Forshay 2020).

Hallouz *et al.* (2018) modeled discharge and solid erosion quantification through a small agricultural watershed by applying the SWAT model on the Wadi Harraza's basin which is part of the Wadi Cheliff's basin to simulate the discharge and sediment concentration for the period from 2004 to 2009. They showed that the SWAT model correctly reproduces and predicts flows over a certain period (2004–2009). Djebou (2018) used SWAT and the Modified Universal Sediment Loss Equation (MUSLE) to quantify spatial variability of sediment loss rates at the watershed scale in a case study for the Somerville reservoir, located in Texas, USA. Watershed behavior and satisfactory values of Nash–Sutcliffe

Efficiency (NSE) were obtained between  $0.76 \leq \text{NSE} \leq 0.69$ . Then the calibrated SWAT was used to generate MUSLE estimates of soil losses under undammed conditions. Meaningful contrasts were outlined between the sub-basins located at the downstream, the midstream, and the upstream.

Tyagi *et al.* (2014) examined the applicability of SWAT in estimating daily discharge and sediment delivery from mountainous forested watersheds named Arnigad and Bansigad, located in India and to assess the impact of forest cover types on stream discharge pattern and sediment load. The results of the study indicated that SWAT is capable of estimating the discharge and sediment yield from Himalayan forested watersheds and can be a useful tool for assessing the hydrology and sediment yield response of the watersheds in the region.

Betrie *et al.* (2011), presented daily sediment yield simulations in the Upper Blue Nile under different Best Management Practice (BMP) scenarios. The model results showed a satisfactory agreement between daily observed and simulated sediment concentrations as indicated by an NSE greater than 0.83. Chandra *et al.* (2014) utilized SWAT for sediment yield estimation in the Burhanpur sub-basin in the Upper Tapi catchment. The average values for NSE and the standard deviation of the measured observations (RSR) for sediment yield were 0.85 and 0.36, respectively, which are within satisfactory limits. Brighenti *et al.* (2019) investigated how and why different calibration methods may affect the uncertainty in flow and sediment estimates. For this purpose, the SWAT model combined with the SUFI-2 algorithm was used. The results were found to be better in concurrent calibration when using King-Gupta Efficiency (KGE) as the objective function, and sequential calibration when using NSE. Ivanoski *et al.* (2019) used SWAT, a GIS-based hydrological model, to study the temporal change of sedimentation rate and to predict sediment production within the Tikvesh reservoir in the southwestern part of the Republic of Macedonia. The results were also compared with information from several bathymetric surveys where the reservoir had a satisfactory match. Martínez-Salvador & Conesa-García (2020) examined the applicability of the SWAT model for the estimation of monthly and annual streamflow and sediment load in the Upper Argos River in the southeast of Spain.

The fit of the simulated annual values was better than that of the monthly values in both cases.

The vast majorities of the studies in the literature were carried out in the middle and downstream sections of the stream. To the best of our knowledge, in the Konya Closed Basin, there is no study in which spatial and temporal analysis of sediment movement is performed. Therefore, it was thought that selection of the Çarşamba Stream Basin, which is an upstream basin as a study area, would constitute a successful example to cover these gaps. Also, when it comes to the regional importance of the study, the Konya Closed Basin is an endorheic basin where it is quite insufficient in terms of water resources, and has a cold-semi-arid climate and intensive agricultural activities. The headwater of the Çarşamba Stream, which is used as a study area, feeds the important water resources at downstream. The inefficiency of the Çarşamba River will cause important water resources and dam reservoirs to lose their effectiveness. Considering its global importance as well as its regional importance, the originality of the study comes to the fore. In this study, the aim was to make a spatial and temporal analysis of the sediment movement for the Çarşamba River upstream basin, which has an important role for the Konya Closed Basin. For this main purpose, objectives were as follows: (i) to establish, calibrate and validate a physically based model for the study area; (ii) to analyze sediment movement as spatially and temporally; and (iii) to suggest strategies for controlling sediment movement to authorities.

## MATERIALS AND METHODS

### Study area and data

The study area covers the drainage area of D16A115 sediment and flow measurement station, which is located in Konya Closed Basin, in Turkey. The altitude of the Çarşamba River varies between 1,100–2,400 m and it has a drainage area of 153.87 km<sup>2</sup>. According to the long-term flow measurement averages, the highest flow rate was observed in April by 6.329 m<sup>3</sup>/s and the lowest flow rate was observed in September by 0.385 m<sup>3</sup>/s. The average of the long-term sediment measurements was identified as

38.4 tons/day. Figure 1 shows the Digital Elevation Model (DEM) and land use-land cover (LULC) map belonging to the study area. The study area is divided into eight sub-basins.

Although short shrubs and rugged terrain are dominant in the study area, there are agricultural and forested areas around the river branches. The Apa Dam, which meets a significant part of the Konya Closed Basin irrigation need, is located downstream of the Çarşamba River. For this reason, investigation of sediment yield downstream of the Çarşamba Stream is getting more significant.

In order to set the SWAT model, meteorological data like precipitation, temperature (maximum and minimum), relative humidity, wind speed and solar radiation have been used. As there was no suitable station that had enough data for modeling inside the study area, the data were taken from Hadim (Station number: 17928) and Seydisehir (Station number: 17898) gauging stations, which are very close to the study basin and operated by the State Meteorological Service. The meteorological data belonging to the study basin were determined by the Thiessen method. Mean maximum temperature, mean minimum temperature and mean annual precipitation were 17.5 °C, 6.1 °C and 785 mm, respectively. The data, which were used for calibrating streamflow and sediment transport rate, were observed from D16A115 streamflow gauging station. The information belonging to the stations used in this study is given in Table 1 and the sediment rating curve of D16A115 streamflow gauging station is given in Figure 2.

### Soil and Water Assessment Tool (SWAT)

The SWAT, which is widely and effectively used in assessing sediment yield, was used in this study. SWAT is a continuous physically based semi-distributed model and an effective tool for assessing changes in hydrological processes developed by Arnold *et al.* (1998). SWAT gives successful results in the determination of agricultural strategies, analyzing sediment transport and sediment yield computations and assessment of pollutant effect on the environment.

In the SWAT model, computations are provided by the Hydrologic Response Units (HRUs). The HRUs, which are unique soil-land use combinations, are defined as the smallest spatial units of the model representing LULC, soil types,

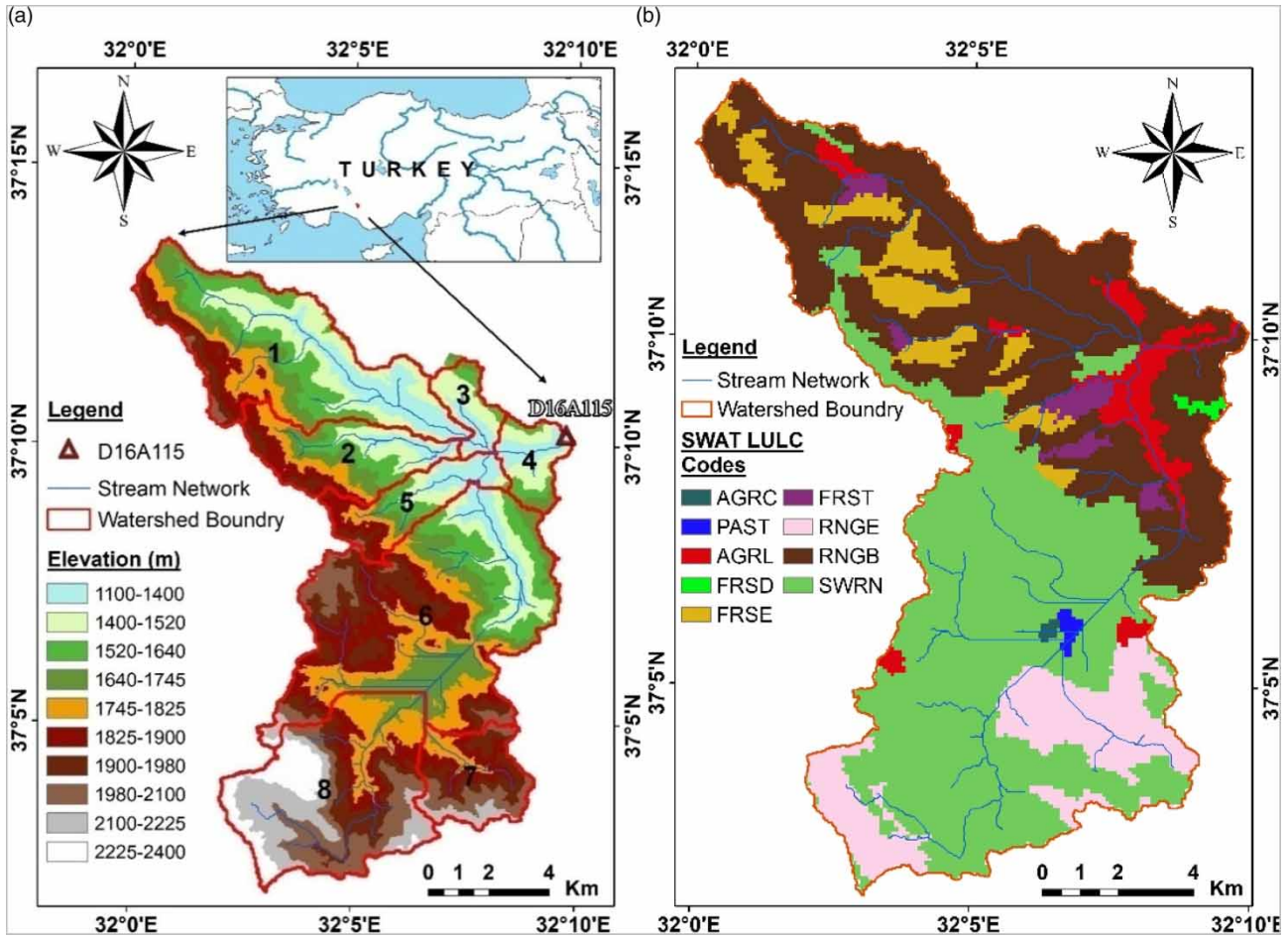


Figure 1 | (a) DEM and (b) LULC map of study area (Koycegiz & Buyukyildiz 2019).

Table 1 | The meteorology and streamflow observation stations used in this study

Station number	Station name	Altitude (m)	Latitude	Longitude
17898	Seydişehir	1,129	37°25'36" N	31°50'56" E
17928	Hadim	1,552	36°59'21" N	32°27'20" E
D16A115	Çarşamba River (Sorkun)	1,150	37°10'12" N	32°09'44" E

and slopes within a sub-basin based upon a user-defined threshold. The user can control the number of HRUs by applying a threshold on land area permitted for given land

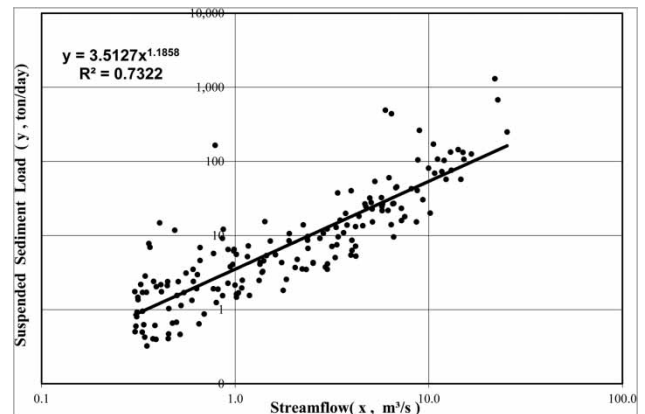


Figure 2 | Sediment rating curve of Çarşamba River-Bozkır (station no. D16A115).

use or soil type within a sub-basin. Mathematical computations of the SWAT model is based on the water balance equations. In the SWAT model, the water balance equation in the hydrological cycle is given as follows:

$$SW_t = SW_0 + \sum_{i=1}^t (R_{day} - Q_{surf} - E_a - W_{seep} - Q_{gw}) \quad (1)$$

where:

$SW_t$ : Final soil water content (mm);

$SW_0$ : Initial soil water content (mm);

$R_{day}$ : Amount of precipitation on a day  $i$  (mm);

$Q_{surf}$ : Amount of surface runoff on a day  $i$  (mm);

$E_a$ : Amount of evapotranspiration on a day  $i$  (mm);

$W_{seep}$ : Amount of percolation and bypass flow exiting the soil profile bottom on a day  $i$  (mm);

$Q_{gw}$ : Groundwater return flow on a day  $i$  (mm).

In this study, the soil conservation services-curve number (SCS-CN) method is used for calculating surface runoff. Easy accessibility to input data, well documentation, production of successful solutions in agricultural areas, and easy integration into the Geographic Information System (GIS) are some of the advantages of the SCS-CN method (Parasuraman et al. 2006). In SWAT, potential evapotranspiration (PET) is calculated using the Penman–Monteith method, which is regarding many agricultural productions' water consumption. Groundwater flow can also be computed by SWAT by considering physical processes separately (Neitsch et al. 2009).

## SWAT model implementation

The SWAT model is used effectively in estimating sediment transport rate, land use management and estimating available water resources in watersheds for various scales and environmental conditions by using topographical data besides meteorological data.

In the SWAT model, meteorological, topographical and land use data are used as input data. SWAT determines the direction of water flow, the borders of the sub-basins and the border of the basins by utilizing a DEM. In this study, DEM maps created from Advanced

Spaceborne Thermal Emission and Reflection Radiometer (ASTER) data were used (Figure 1(a)). The soil map for analyzing groundwater flow was taken by the Harmonized World Soil Database v1.2 (HWSD v1.2). The LULC map needed for successful modeling of surface water and infiltration and used for the SWAT model was derived from the Coordination of Information on the Environment (CORINE) data (Figure 1(b)).

The study area was divided into eight sub-basins. SWAT codes and areas for LULC are seen in Table 2.

The dominant LULC is seen as SWRN having 41% in the overall area. It is followed by RNGB and RNGE with 34% and 14%, respectively. The rest of the LULC is not classified as their ranges are small and given totally as 14%. If Figure 3 is analyzed, it can be seen that sub-basins have various LULC distributions. Dominant LULC is an RNGB of 73, 64, 79 and 71% belonging to sub-basins 1, 2, 3 and 4, respectively. The sub-basins 5, 6 and 8 have SWRN as the dominant LULC of %43, %61 and %72, respectively. This figure indicates that RNGE is the dominant LULC of 59% in sub-basin 7. In addition, there is a more complex LULC pattern as shown in sub-basin 5 compared with other sub-basins. While FRSE occupied intensively the 1st and 2nd sub-basins, FRST occupies a very large area only in the 5th sub-basin. It was observed that AGRL occupied more than a 10% area in sub-basins of 3th, 4th and 5th sub-basins.

Generally, there are three soil types in the study area. Soil types belonging to sub-basins and overall study area are given in Figure 4. Soil types in the basin consisted of

**Table 2** | Soil and water assessment tool (SWAT) codes and areas for LULC

SWAT LULC codes	Definition of SWAT LULC codes	Area (km <sup>2</sup> )	Area (%)
AGRC	Agricultural Land-Close Grown	0.24	0.16
PAST	Pasture	0.50	0.32
AGRL	Agricultural Land-Generic	7.61	4.94
FRSD	Forest-Deciduous	0.42	0.27
FRSE	Forest-Evergreen	9.46	6.14
FRST	Forest-Mixed	3.22	2.09
RNGE	Range-Grasses	16.32	10.60
RNGB	Range-Brush	52.97	34.42
SWRN	South Western Range-Bare Rock	63.1	41.00

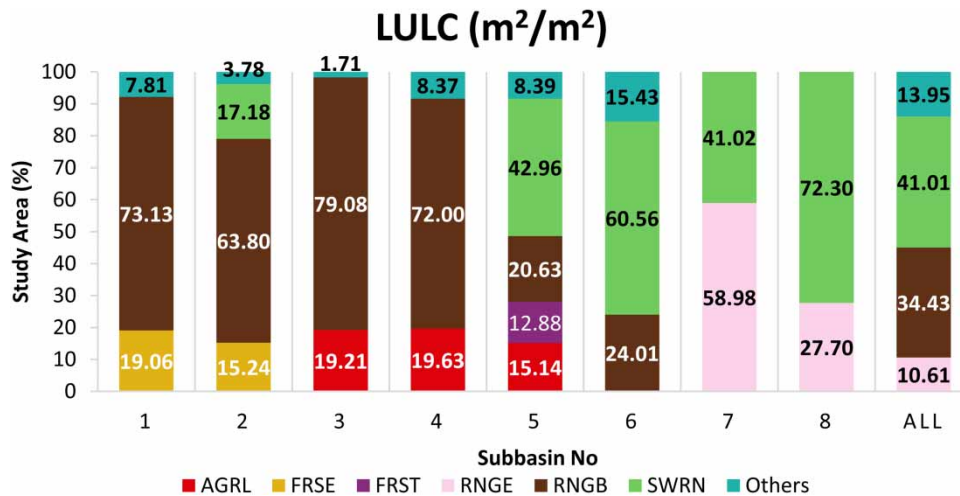


Figure 3 | LULC of the study area.

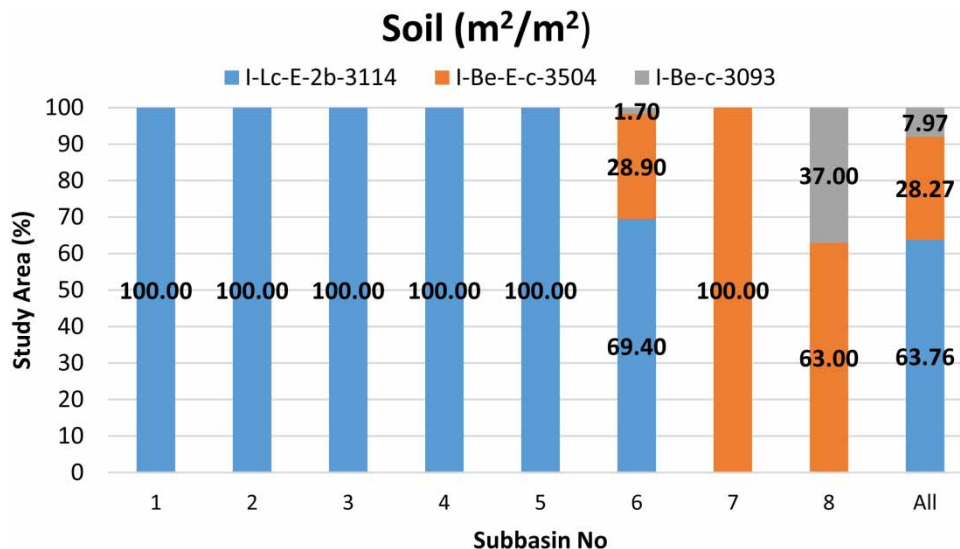


Figure 4 | Soil types of the study area.

Lithosol (I), Eutric Cambisol (Be), Luvisol (Lc), and Rendzina (E). If the basin is considered as a whole, the soil type I-Lc-E-2b-3114 code is dominant with 64% of the study area. It is followed by I-Be-E-c-3504 and I-Be-c-3093 codes with 28 and 8%, respectively. There is only the I-Lc-E-2b-3114 code soil type that covers the 1–5 sub-basins. There is only the I-Be-E-c-3504 code soil type in the 7th sub-basin. The most common soil type is Be-c-3093 code at 37% in the 8th sub-basin. The only sub-basin which was observed to have considerable amounts of all soil types was

the 6th sub-basin. In this basin, lithosol is the dominant soil type, which is shallow soil consisting of imperfectly weathered rock fragments, in the basin (Koycegiz & Buyukyildiz 2019). Its structure is very important in sediment transport as it can be eroded easily and excessively drained or is highly resistant to the soil-forming processes.

Figure 5 shows the variation of the slopes of the study area. Slope variations are divided into 5 as 0–15%, 15–24%, 24–35%, 35–49% and higher than 49%. It can be concluded from this figure that a steep slope is dominant

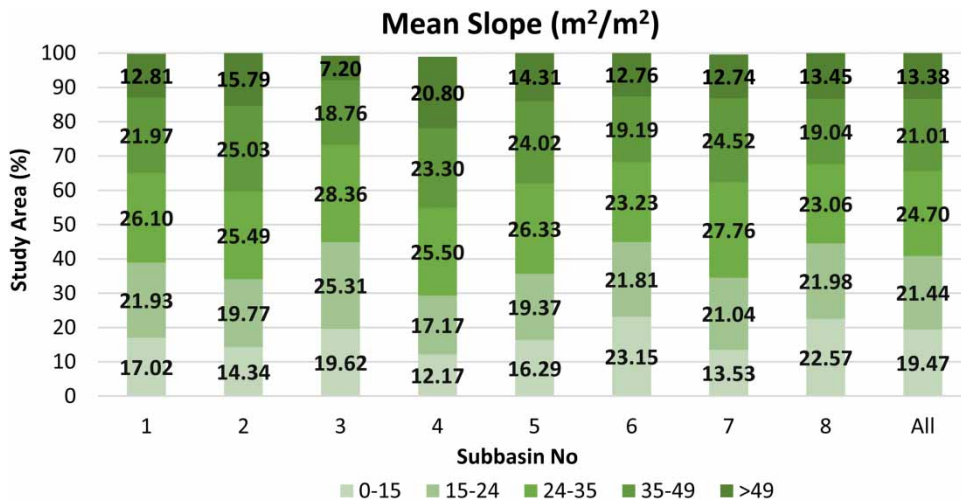


Figure 5 | Slope classes in the study area.

in the basin. Most of the basin (59% of the basin) is steeper than 25%. If the basin is considered, 0–15%, 15–24%, 24–35%, 35–49% and >49 slopes are shared out as 19, 21, 25, 21 and 13%, respectively. If the basin is considered overall, a slope of 24.7% is seen the most. While the 4th and the 7th sub-basins have steeper slopes, the 3rd, 6th and 8th sub-basins have gentler slopes than the other sub-basins.

If the sub-basins are analyzed, the steepest one is the 4th sub-basin, which is steeper than 25% in 71% of its area. It is followed by the 2nd, 5th and 7th sub-basins, in which 66% is steeper than 25%.

The majority of the study area is covered by mountainous and has steep slopes. So it is expected that sediment transport rate significantly increases because of the erosion of the land surface.

### Sediment model

The Modified Universal Soil Loss Equation (MUSLE) was used to calculate the sediment yield (Williams 1975a, 1975b). The main advantages of the MUSLE method are that it is simple to implement and includes concepts of different physical processes. It also can incorporate management strategies into the model. The runoff factor in the MUSLE method increases the sediment estimation capacity. The fact that runoff is a function of not only precipitation energy but also previous humidity conditions increases success in

estimating sediment yield (Neitsch et al. 2009). The sediment yield calculated with MUSLE is given in Equation (2):

$$sed = 11.8 (Q_{surf} \cdot q_{peak} \cdot area_{hru})^{0.56} \cdot K_{USLE} \cdot P_{USLE} \cdot C_{USLE} \cdot LS_{USLE} \cdot CFRG \quad (2)$$

where sed is the sediment yield, CFRG is the coarse fragment factor,  $area_{hru}$  is an area of the HRU,  $Q_{surf}$  is surface runoff volume,  $q_{peak}$  is the peak runoff rate,  $K_{USLE}$  is Universal Sediment Loss Equation (USLE) soil erodibility factor,  $P_{USLE}$  is USLE support practice factor,  $C_{USLE}$  is USLE cover and management factor, and  $LS_{USLE}$  is USLE topographic factor (Neitsch et al. 2009).

### Calibration and validation

In this study, automatic calibration and validation steps were performed using Sequential Uncertainty Fitting Version 2 (SUFI-2) included in the SWAT-CUP program. The SUFI-2 algorithm is frequently preferred due to its advantages in calibration and uncertainty analysis processes (Khoi & Thom 2015). In SUFI-2, the uncertainty of the parameters is expressed as a range corresponding to the uncertainty of all variables. The algorithm takes into account the uncertainties of the parameters, the theoretical infrastructure of the model and the measured data. The spread of uncertainty creates a confidence interval. For the SUFI-2 algorithm, a range (95PPU) containing the most suitable solutions at a 95% significance level is obtained as a result. Also, the specified

confidence interval is intended to include the measured data. With the SUFI-2 algorithm, two different statistics are taken into account during the solution phase. The first is the P-factor and the second is the R-factor. The P-factor is the percentage of actual data covered by the 95PPU. The R-factor is the thickness of the 95PPU range. The algorithm works on the principle of obtaining the most P-factor with the least R-factor. Theoretically, the P-factor ranges between 0 and 100%, and the R-factor ranges between 0 and infinity. In cases where the P-factor is 100% and the R-factor is 0, the simulation data overlap with the measured data.

### Performance criteria

In this study, Root Mean Square Error (RMSE), Mean Absolute Error (MAE), Determination Coefficient ( $R^2$ ), Nash–Sutcliffe Efficiency Coefficient (NSE) and Percent Bias (PBIAS) were used as performance criteria in evaluating the success of the sediment prediction model obtained with SWAT (Nash & Sutcliffe 1970; Madsen 2000; Krause et al. 2005; Zhang et al. 2011; Pokhrel et al. 2012). Moriasi et al. (2007), gave performance rates for NSE,  $R^2$  and PBIAS (Table 3).

## RESULTS AND DISCUSSION

In this study, the SWAT model was simulated from 2003 to 2015. While the period from 2003 to 2005 was used for the warm-up, the periods from 2006 to 2011 and from 2012 to 2015 were used for calibration and validation, respectively. The sediment rating curve of this station (Figure 2) was used to complete the missing sediment data of the station used in the study. The study area was divided into eight sub-basins and the SUFI-2 algorithm in SWAT-CUP was used for model calibration and validation. The hydrology

model of the basin was created and calibrated before the sediment model was created. The hydrology model has been evaluated with different performance criteria, but NSE has been taken into account as an objective function. After the development of the hydrology model, the sediment model was calibrated. Here, 20 important parameters representing the physical processes were chosen for calibration for the successful creation of the sediment model. The parameters to be calibrated, the range of values they can take and the values of the calibrated parameters are given in Table 4.

The performance metrics obtained after the calibration phase of the sediment model are given in Table 5 for both streamflow and sediment. According to Table 5, as a result of the SWAT model, a very good performance was obtained with the values  $R^2 = 0.787$ ,  $NSE = 0.779$  and  $PBIAS = -7.562\%$  for the streamflow data during the calibration period. In the validation period, model success was achieved satisfactorily with  $R^2 = 0.508$ ,  $NSE = 0.502$ , and very good with  $PBIAS = -8.163\%$ . According to the SWAT-sediment model results in Table 5, performance metrics were obtained as  $R^2 = 0.68$ ,  $NSE = 0.68$  and  $PBIAS = -3.04\%$  for calibration, and  $R^2 = 0.76$ ,  $NSE = 0.66$  and  $PBIAS = 15.48\%$  for validation. According to the literature, the results obtained with the SWAT model indicated that the sediment model was successful (Moriasi et al. 2007). The SWAT model, which was created according to the  $R^2$  and NSE results obtained, was more successful in estimating the amount of streamflow in the calibration period, while it was more successful in estimating the amount of sediment in the validation period. In addition, the SWAT model yielded an underestimation (overestimation) with negative (positive) PBIAS value during the calibration (validation) period in sediment estimation, and underestimation with negative PBIAS values in both periods for streamflow estimation. The underestimation and overestimation states of

**Table 3** | General performance ratings (Moriasi et al. 2007)

Performance rating	NSE	$R^2$	PBIAS (%)	
			Streamflow	Sediment
Very Good (VG)	$0.75 < NSE \leq 1.00$	$0.75 < R^2 \leq 1.00$	$PBIAS < \pm 10$	$PBIAS < \pm 15$
Good (G)	$0.65 < NSE \leq 0.75$	$0.65 < R^2 \leq 0.75$	$\pm 10 \leq PBIAS < \pm 15$	$\pm 15 \leq PBIAS < \pm 30$
Satisfactory (S)	$0.50 < NSE \leq 0.65$	$0.50 < R^2 \leq 0.65$	$\pm 15 \leq PBIAS < \pm 25$	$\pm 30 \leq PBIAS < \pm 55$
Unsatisfactory (U)	$NSE \leq 0.50$	$R^2 \leq 0.50$	$PBIAS \geq \pm 25$	$PBIAS \geq \pm 55$

**Table 4** | The parameters and values used in the sediment calibration

Parameters	Parameter definitions	Range	Fitted value
V_SPCON.bsn	Linear parameter for calculating the maximum amount of sediment that can be reentrained during channel sediment routing	0.0001–0.01	0.0003
V_SPEXP.bsn	Exponent parameter for calculating sediment reentrained in channel sediment routing	1–1.5	1.00
V_CH_ERODMO.rte	Jan. channel erodability factor	0–1	0
V_CH_COV1.rte	Channel erodibility factor	– 0.05–0.6	0
V_CH_COV2.rte	Channel cover factor	– 0.001 to 1	0
V_ADJ_PKR.bsn	Peak rate adjustment factor for sediment routing in the sub-basin (tributary channels)	0.5–2	1.00
V_C_FACTOR.bsn	Scaling parameter for cover and management factor in ANSWERS erosion model	0.001–0.45	0.030
V_USLE_P.mgt	USLE equation support practice factor	0–1	1.00
V_USLE_K.sol	USLE equation soil erodibility (K) factor	0–0.65	0.2449
V_RSDCO.bsn	Residue decomposition coefficient	0.02–0.1	0.050
V_BIOMIX.mgt	Biological mixing efficient	0–1	0.2
R_CH_WDR.rte	Channel width-depth ratio	0–10,000	27.169
V_CH_BED_KD.rte	Erodibility of channel bed sediment by jet test ( $\text{cm}^3/\text{N}\cdot\text{s}$ )	0.001–3.75	3.16
V_CH_BNK_KD.rte	Erodibility of channel bank sediment by jet test ( $\text{cm}^3/\text{N}\cdot\text{s}$ )	0.001–3.75	2.08
V_CH_BNK_D50.rte	D50 Median particle size diameter of channel bank sediment	1–10,000	4,250.57
V_CH_BNK_TC.rte	Critical shear stress of channel bank ( $\text{N}/\text{m}^2$ )	0–400	130
V_CH_BNK_BD.rte	Bulk density of channel bank sediment ( $\text{g}/\text{cc}$ )	1.1–1.9	1.48
V_CH_BED_BD.rte	Bulk density of channel bed sediment ( $\text{g}/\text{cc}$ )	1.1–1.9	1.87
V_CH_BED_D50.rte	D50 Median particle size diameter of channel bed sediment	1–10,000	8,150.18
V_SLSUBBSN.hru	Average slope length	10–150	21.303

**Table 5** | The performance of the SWAT model in the calibration and validation of the streamflow and sediment simulation

Performance criteria	Streamflow (Koycegiz & Buyukyildiz 2020)		Sediment	
	Calibration	Validation	Calibration	Validation
$R^2$	0.787 (VG)	0.508 (S)	0.68 (G)	0.76 (VG)
NSE	0.779 (VG)	0.502 (S)	0.68 (G)	0.66 (G)
PBIAS (%)	– 7.562 (VG)	– 8.163 (VG)	– 3.04 (VG)	15.48 (G)
RMSE	0.962 $\text{m}^3/\text{s}$	1.334 $\text{m}^3/\text{s}$	7.20 ton/day	48.52 ton/day
MAE	0.645 $\text{m}^3/\text{s}$	0.917 $\text{m}^3/\text{s}$	5.24 ton/day	3.27 ton/day

both parameters for both the calibration and validation period can be seen in Figure 6.

The observed and simulated daily streamflow and sediment yield during the calibration period of 2006–2011 and the validation period of 2012–2015 are graphically presented in Figure 5. The peak streamflow during the observation period was generally obtained in the February–May period. However, the peak streamflow that started in

February 2011 and 2015 continued until July. It is seen that the highest flow was achieved as  $20.75 \text{ m}^3/\text{s}$  in 2011. When the sediment data in Figure 5 are analyzed, it is seen that the highest sediment yield was simulated as 214.3 ton/day in 2012. According to Figure 5, the shape of the streamflow and sediment yield is almost the same.

The annual averages of sediment inflow and sediment outflow amounts in the sub-basins are given in Figures 7

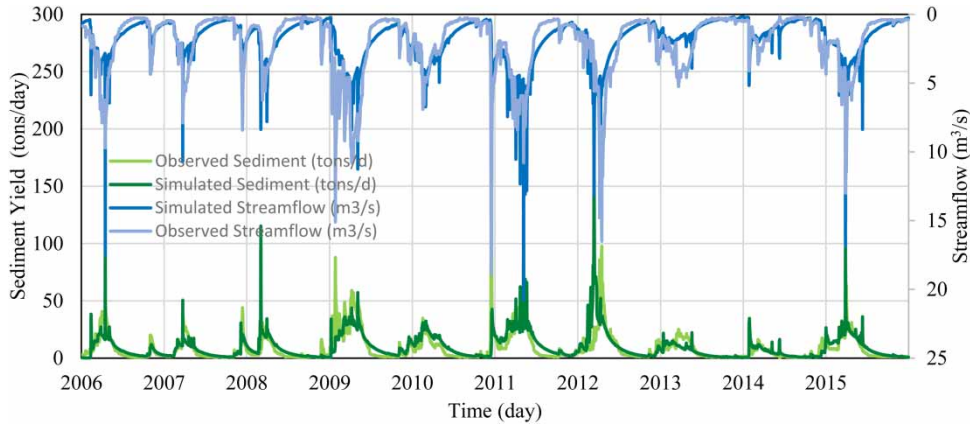


**Figure 6** | Observed and simulated streamflow and sediment yield in the model calibration and validation period.

and 8, respectively. There is no sediment inflow into the 1st, 2nd, 7th and 8th sub-basins from another basin. These basins transfer the amount of sediment they produce to the next basins. The 3rd, 4th, 5th and 6th sub-basins receive sediment from the sub-basins in the upper parts of the stream. The 6th

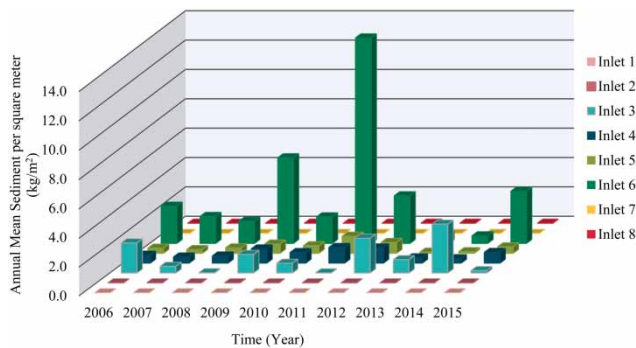


**Figure 7** | Annual sediment inflow per sub-basins (per square meter).

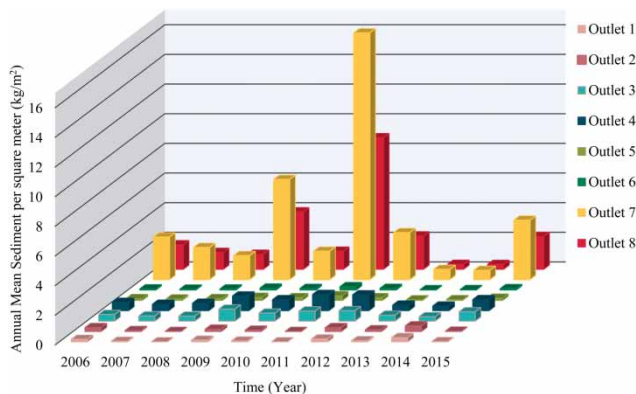


**Figure 8** | Annual sediment outflow per sub-basins (per square meter).

sub-basin was determined as the sub-basin that received the most sediment. The most sediment inflow to this sub-basin was in 2011 with approximately  $12.5 \text{ kg/m}^2$ .

According to Figure 8, it is seen that there is more sediment outflow in the 7th and 8th sub-basins than the other sub-basins. High sediment outflows were observed in these sub-basins in 2009 and 2011 compared to other years. The slope and land cover of the 7th and 8th lower basins are thought to cause this situation. Steep slopes are higher in these basins compared to other basins. In addition, they have a land cover in which bare rocks are dense without dense vegetation. In the sub-basins to the north of the study area, a land cover dominated by the bush is dominant. In addition, forests and agricultural lands are densely located in the north of the basin. Sediment is kept in the 6th sub-basin. There is no significant sediment outflow in the sub-basins up to 1 and 6. Land cover of these basins largely prevents erosion during precipitation.

## CONCLUSION

In this study, sediment yield was investigated temporally and spatially for Çarşamba Stream in Konya Closed Basin. Warm-up, calibration and validation periods were evaluated for years 2003–2005, 2006–2012, 2013–2015 respectively. The sediment model was established and calibrated on the developed hydrology model. The model was calibrated using the SUFI-2 algorithm. Calibration was made with 20 sensitive parameters taking into account the important physical processes affecting the sediment model. Deficiencies in

sediment data were obtained from the sediment rating curve of the station (D16A115).

- As a result of the study, a successful sediment model has been developed.  $R^2 = 0.68$ ,  $NSE = 0.68$  values in the calibration period;  $R^2 = 0.76$  and  $NSE = 0.66$  values in the validation period were obtained.
- During the observation period, high sediment yields and high flow rates were determined in 2011 and 2012. The increase in sediment yield during periods when high flows are observed during the year shows that the flow has a significant correlation with sediment.
- It was determined that sediment production was not significant in 1–6 sub-basins. It is thought that the bushes and forests in the land cover have a positive effect on this situation.
- There is a significant amount of sediment inflow from the 7th and 8th sub-basins to the 6th sub-basin. However, the 6th sub-basin holds a large part of the sediment it receives. This is an important factor in explaining the fact that there are more slightly sloping areas in the 6th sub-basin and the increase of shrubs, agricultural land and forests in the land cover north of the sub-basin.
- Looking at the whole basin, the fact that the dominant soil type is one of the easily degradable soil classes, lithosols, shows that the basin has a soil structure prone to sediment production.
- In 2009 and 2011, quite a lot of sediment production was observed in the 7th and the 8th sub-basins compared with other years.

By the obtained results, it was determined that the 7th and 8th sub-basins in the southern basin produced a significant amount of sediment. It was evaluated that this situation is caused by the slope and land cover characteristics of these basins. The sediment transmitted from the Çarşamba Stream upstream affects the lifetime of the Apa Dam, which is an important water source for the Konya Closed Basin. In the short term, the fact that the 6th lower basin holds a large part of the sediment coming from the other sub-basins in the upper parts may create the impression that there is no problem. However, in the long term, the river structure of the 6th sub-basin is foreseen to show significant changes with sediment accumulating. Changing river structure may affect flow efficiency negatively or cause floods to occur.

The solutions and research suggestions that can be developed for the sediment accumulation problem in the sixth basin are given below.

- Terracing can be done in places where the slope is high in the south of the basin.
- Considering the environmental effects and soil properties, priority should be given to the cultivation of plants that can prevent surface erosion in accordance with the climate of the region.
- In line with the changing precipitation and temperature values under climate change, erosion in the basin will also change. An accurate sediment management strategy can be developed by making future projections.

## FUNDING

This research did not receive any specific grant from funding agencies in the public, commercial, or not-for-profit sectors.

## DATA AVAILABILITY STATEMENT

Data cannot be made publicly available; readers should contact the corresponding author for details.

## REFERENCES

- Akar, T. & Aksoy, H. 2020 [Stochastic and analytical approaches for sediment accumulation in river reservoirs](#). *Hydrological Sciences Journal* **65** (6), 984–994.
- Arnold, J. G., Srinivasan, R., Muttiah, R. S. & Williams, J. R. 1998 [Large area hydrologic modelling and assessment part I: model development](#). *Journal of The American Water Resources Association* **34** (1), 73–89.
- Azzellino, A., Cevirgen, S., Giupponi, C., Parati, P., Ragusa, F. & Salvetti, R. 2015 [SWAT meta-modeling as support of the management scenario analysis in large watersheds](#). *Water Science and Technology* **72** (12), 2103–2111.
- Betrie, G. D., Mohamed, Y. A., van Griensven, A. & Srinivasan, R. 2011 [Sediment management modelling in the Blue Nile Basin using SWAT model](#). *Hydrology and Earth System Sciences* **15**, 807–818.
- Borah, D. K. & Bera, M. 2003 [Watershed-scale hydrologic and nonpoint-source pollution models: review of mathematical bases](#). *Transactions of the ASABE* **46** (6), 1553–1566.

- Brighenti, T. M., Bonumá, N. B., Grison, F., Mota, A. A., Kobiyama, M. & Chaffe, P. L. B. 2019 Two calibration methods for modeling streamflow and suspended sediment with the SWAT model. *Ecological Engineering* **127**, 103–113.
- Chandra, P., Patel, P. L., Porey, P. D. & Gupta, I. D. 2014 Estimation of sediment yield using SWAT model for Upper Tapi basin. *Journal of Hydraulic Engineering* **20** (3), 291–300.
- Dogan, E. 2009 Katı Madde Konsantrasyonunun Yapay Sinir Ağlarını Kullanarak Tahmin Edilmesi. *İMO Teknik Dergi* **20** (96), 4567–4582.
- Hallouz, F., Meddi, M., Mahé, G., Alirahmani, S. & Keddar, A. 2018 Modeling of discharge and sediment transport through the SWAT model in the basin of Harraza (northwest of Algeria). *Water Science* **32**, 79–88.
- Ivanoski, D., Trajkovic, S. & Gocic, M. 2019 Estimation of sedimentation rate of Tikvesh Reservoir in Republic of Macedonia using SWAT. *Arabian Journal of Geosciences* **12**, 438.
- Kesikoglu, M. H., Atasever, U. H., Dadaser-Celik, F. & Ozkan, C. 2019 Performance of ANN, SVM and MLH techniques for land use/cover change detection at Sultan Marshes wetland, Turkey. *Water Science and Technology* **80** (3), 466–477.
- Khoi, D. N. & Thom, V. T. 2015 Parameter uncertainty analysis for simulating streamflow in a river catchment of Vietnam. *Global Ecology and Conservation* **4**, 538–548.
- Koycegiz, C. & Buyukyildiz, M. 2019 Calibration of SWAT and two data-driven models for a data-scarce mountainous headwater in semi-arid Konya Closed Basin. *Water* **11** (1), 1–17.
- Krause, P., Boyle, D. P. & Bäse, F. 2005 Comparison of different efficiency criteria for hydrological model assessment. *Advances in Geosciences* **5**, 89–97.
- Madsen, H. 2000 Automatic calibration of a conceptual rainfall–runoff model using multiple objectives. *Journal of Hydrology* **235** (3), 276–288.
- Mahmood, K. 1987 *Reservoir Sedimentation: Impact, Extent, Mitigation*. World Bank Tech. Rep, Washington, DC.
- Martínez-Salvador, A. & Conesa-García, C. 2020 Suitability of the SWAT model for simulating water discharge and sediment load in a karst watershed of the semiarid Mediterranean basin. *Water Resources Management* **34**, 785–802.
- Moriasi, D., Arnold, J., Van Liew, M., Bingner, R., Harmel, R. & Veith, T. 2007 Model evaluation guidelines for systematic quantification of accuracy in watershed simulations. *Transactions of the ASABE* **50** (3), 885–900.
- Nash, J. E. & Sutcliffe, J. V. 1970 River flow forecasting through conceptual models: part 1. A discussion of principles. *Journal of Hydrology* **10** (3), 282–290.
- Neitsch, S. J., Arnold, J. G., Kiniry, J. R. & Williams, J. R. 2009 *Soil and Water Assessment Tool Theoretical Documentation Version 2009*. College of Agriculture and Life Sciences. Texas A&M University System: College Station, USA.
- Öztürk, F., Apaydın, H. & Walling, D. E. 2001 Suspended sediment loads through flood events for streams of Sakarya Basin. *Turkish Journal of Engineering and Environmental Sciences, TUBITAK* **25**, 643–650.
- Parasuraman, S. B., Mishra, S. & Singh, V. P. 2006 *SCS-CN Method Revisited. Advances in Hydraulics and Hydrology*. Water Resources Publication Colorado.
- Pokhrel, P., Yilmaz, K. & Gupta, H. 2012 Multiple-criteria calibration of a distributed watershed model using spatial regularization and response signatures. *Journal of Hydrology* **418–419**, 49–60.
- Ricci, G. F., De Girolamo, A. M., Abdelwahab, O. M. M. & Gentile, F. 2018 Identifying sediment source areas in a Mediterranean watershed using the SWAT model. *Land Degradation and Development* **29**, 1233–1248.
- Sivakumar, B. 2006 Suspended sediment load estimation and the problem of inadequate data sampling: a fractal view. *Earth Surface Process Landforms* **31**, 414–427.
- Sohoulane-Djebou, D. C. 2018 Assessment of sediment inflow to a reservoir using the SWAT model under undammed conditions: a case study for the Somerville reservoir, Texas, USA. *International Soil and Water Conservation Research* **6**, 222–229.
- Tyagi, J. V., Rai, S. P., Qazi, N. & Singh, M. P. 2014 Assessment of discharge and sediment transport from different forest cover types in lower Himalaya using Soil and Water Assessment Tool (SWAT). *International Journal of Water Resources and Environmental Engineering* **6** (1), 49–66.
- Yuan, L. & Forshay, K. J. 2020 Using SWAT to evaluate streamflow and lake sediment loading in the Xinjiang River Basin with limited data. *Water* **12** (1), 39.
- Williams, J. R. 1975a Sediment-yield prediction with universal soil equation using runoff energy factor. In: *Present and Prospective Technology for Predicting Sediment Yield and Sources*, Oxford, pp. 244–252.
- Williams, J. R. 1975b Sediment routing for agricultural watersheds. *Journal of the American Water Resources Association* **11** (5), 965–974.
- Zeiger, S. J. & Hubbart, J. A. 2016 A SWAT model validation of nested-scale contemporaneous stream flow, suspended sediment and nutrients from a multiple-land-use watershed of the central USA. *Science of the Total Environment* **572**, 232–243.
- Zhang, H., Huang, G. H., Wang, D. & Zhang, X. 2011 Multi-period calibration of a semi-distributed hydrological model based on hydroclimatic clustering. *Advances in Water Resources* **34** (10), 1292–1303.

First received 13 November 2020; accepted in revised form 5 January 2021. Available online 19 January 2021